Available online at www.sciencedirect.com
SCIENCE DIRECT
Polymer 46 (2005) 4596–4603
polymer
www.elsevier.com/locate/polymer

Composite magnetic particles: 2. Encapsulation of iron oxide by surfactant-free emulsion polymerization

A. Pich[a,*], S. Bhattacharya[a], A. Ghosh[b], H.-J.P. Adler[a]

[a]*Institute of Macromolecular Chemistry and Textile Chemistry, Dresden University of Technology, D-01062 Dresden, Germany*
[b]*Indian Institute of Technology, Delhi, India*

Received 8 September 2004; received in revised form 3 January 2005; accepted 3 January 2005

Abstract

This is a second paper in the series concerning the synthesis and characterization of composite polymeric particles with encapsulated magnetic iron oxide and bearing reactive β-diketone groups on the surface. Composite particles have been prepared by two-step method in which first step requires preparation of the iron oxide nano-particles and during second step iron oxide was encapsulated into formed poly(styrene/acetoacetoxyethyl methacrylate) (PS-AAEM) particles directly during polymerization process. It has been found that the modification of the iron oxide nano-particle surface with sodium oleate improves significantly the encapsulation during polymerization process. This procedure gives a possibility to obtain composite particles with raspberry morphology and both the particle size and iron oxide content can be varied. Change of monomer to iron oxide ratio gives a possibility to change effectively the morphology of hybrid particles, however, polydispersity of composite particles increases at higher content of magnetic particles in the system. Variation of AAEM concentration in reaction mixture at constant iron oxide particles concentration gives a possibility to control the particle size of formed hybrid microspheres. Composite particles were characterized by dynamic light scattering and electron microscopy (SEM) with respect to their particle size and morphology of the surface layer. X-ray diffraction (XRD) and magnetization measurements indicate presence of maghemite (γ-Fe_2O_3) in composite particles.

Keywords: Iron oxide; Hybrid latex particles

1. Introduction

There is a considerable interest in preparation of particles which can be manipulated in different systems by external stimuli such as thermal, electric or magnetic field. Polymeric particles can be easily prepared and their size, morphology and surface groups can be varied in the broad range. However, conventional polymers cannot provide some special properties like, for example magnetic response. Therefore, incorporation of magnetic iron oxides in polymeric particles can be an interesting route for preparation of hybrid particles which can provide this interesting feature.

Various strategies have been proposed for synthesis of magnetic polymer particles [1]. Ugelstad and co-workers developed a novel method based on a two-step swelling technique and successfully prepared monodisperse magnetic microspheres [2,3].

Recently the layer-by-layer deposition technique was developed by Caruso and co-workers [4,5] to prepare functionalized microcapsules from oppositely charged polyelectrolytes with loaded magnetite.

The stepwise heterocoagulation method has been successfully used by Furusawa et al. [6] and Sauzedde et al. [7,8] to form magnetic particles by coagulation of two different colloids one of them being magnetic. Sauzedde et al. [7,8] developed a three-step procedure which requires (a) synthesis of different seed particles (polystyrene, poly (styrene/*N*-isopropylacrylamide) and poly (*N*-isopropylacrylamide), (b) adsorption of magnetic nano-particles on the seed particle surface, and finally (c) seed precipitation polymerization of *N*-isopropylacrylamide. Authors obtain

* Corresponding author.
E-mail address: andrij.pich@chemie.tu-dresden.de (A. Pich).

0032-3861/$ - see front matter © 2005 Elsevier Ltd. All rights reserved.
doi:10.1016/j.polymer.2005.01.017

superparamagnetic, hydrophilic microspheres with various dimensions and magnetite contents. Dresco et al. [9] reported preparation of magnetic polymeric nano-particles by synthesis of magnetite core and polymeric shell in a single inverse microemulsion. The polymerization of methacrylic acid, hydroxyethyl methacrylate and cross-linker lead to formation of stable hydrophilic polymeric shell. Recently Gu et al. [10] reported a novel method for preparation of magnetic latex particles. In this approach coating of polymer particles with surface-modified magnetic particles with silane reagents occurs during soap-free emulsion polymerization. Condensation of SiOH groups on the magnetic and polymeric particles followed by polymerization of vinyl bonds lead to formation of hybrid particles with different morphologies. Elaissari et al. [11] designed a new strategy for preparation of magnetic particles requiring no final polymerization step. In this approach small film-forming positively charged nano-particles coagulate on the surface of negatively charged magnetic particles and form a polymeric shell when heated above their T_g. In this way also fluorescent particles have been incorporated into polymeric shell and hybrid particles with high iron oxide content have been obtained.

In previous paper [12], we described synthesis of PS-AAEM polymeric particles by surfactant-free emulsion polymerization. Monodisperse latex articles functionalized with β-diketone groups have been obtained and characterized. Since β-diketone groups are capable to chelate effectively metal ions, obtained polymeric particles have been used as templates for iron oxide deposition what leads to formation of hybrid core-shell composites. Present paper summarises the results about formation of hybrid particles *in situ* by encapsulation of pre-formed iron oxide nano-particles during surfactant-free emulsion polymerization of styrene (ST) and acetoacetoxyethyl methacrylate (AAEM).

2. Experimental part

2.1. Materials

Styrene (ST) (from Fluka) and acetoacetoxyethyl methacrylate (97%) (AAEM) (from Aldrich) were purified by conventional methods and then vacuum distilled under nitrogen. Sodium peroxydisulfate (97%) (SPDS) and 2,2′-azobis(2-methylpropyonamidine) dihydrochloride (97%) (AMPA), iron (III) chloride ($FeCl_3$), iron (II) chloride ($FeCl_2$), and sodium oleate were received from Aldrich and used as commercially available. Ammonium hydroxide (NH_4OH) in form of 40% water solution was obtained from Fluka. Distilled water was employed as polymerization medium.

2.2. Synthesis of iron oxide particles

Solutions of $FeCl_2$ and $FeCl_3$ were prepared in separate flasks and added to stirred dispersion under nitrogen blanket (molar ratio $FeCl_3$:$FeCl_2$ was kept constant at 2:1). Water solution of NH_4OH was added drop-wise to start iron oxide formation process. Immediately after base addition solution became dark-brown indicating that iron oxide has been formed in the system. After 30 min formed composite particles were removed from reaction vessel and cleaned by precipitation to remove all by-products. Magnetic nano-particles were washed with 0.01 M HCl solution. Magnetic dispersion with HCl solution was centrifuged (Universal 16 A) at a speed of 3000 U/min for 25 min to precipitate the particles. This procedure was repeated for four times. After that precipitated magnetic particles were cleaned with distilled water. Then calculated amount of sodium oleate was added to the required amount of magnetic dispersion (15 mg Na-oleate in 50 ml of 1.1 mg/ml magnetic dispersion, keeping the ratio constant at 1:1). Then the dispersion was heated to 80 °C for 5 min and finally sonified for another 5 min.

2.3. Synthesis of PS/AAEM/Iron oxide particles

Double-wall glass reactor equipped with stirrer and reflux condenser was purged with nitrogen. Appropriate amounts of iron oxide dispersion (from 0.92 to 9.2 g) were diluted with water to keep the total water amount 20 g and then ST (1.33 g) and AAEM (0.07 g, 5% to ST) were added into reactor and stirred at room temperature. After 10 min temperature was increased to 70 °C and water solution of initiator (0.07 g in 2 g water) was added to start the polymerization process.

2.4. Analytical methods

2.4.1. Particle size analysis

A commercial laser light scattering (LLS) spectrometer (ALV/DLS/SLS-5000) equipped with an ALV-5000/EPP multiple digital time correlator and laser goniometer system ALV/CGS-8F S/N 025 was used with a helium-neon laser (Uniphase 1145P, output power of 22 mW and wavelength of 632.8 nm) as the light source.

In dynamic LLS, the intensity-intensity-time correlation function $g_2(q,t)$ in the self-beating mode was measured and can be expressed by the Siegert relation:

$$g_2(q,t) = A(1 + \beta|g_1(q,t)|^2) \quad (1)$$

where t is the decay time, A is a measured baseline, β is the coherence factor, and $g_1(q,t)$ is the normalized first-order electric field time correlation function and $g_1(q,t)$ is related to the measured relaxation rate Γ:

$$g_1(q,t) = G(\Gamma)\exp(-\Gamma t)d\Gamma \quad (2)$$

A line-width distribution $G(\Gamma)$ can be obtained from the Laplace inversion of $g_1(t)$ (CONTIN procedure) [10]. For a pure diffusive relaxation, Γ is related to the translational

diffusion coefficient D at $q \to 0$ and $c \to 0$ by

$$D = \Gamma/q^2 \quad (3)$$

or a hydrodynamic radius R_h given by

$$R_h = k_B T/(6\pi\eta D) \quad (4)$$

with q, k_B, T and η being scattering vector, the Boltzman constant, absolute temperature, and solvent viscosity, respectively. All DLS experiments were carried out at angles $\theta = 30$–$140°$. The sample in a 10 mm test tube was immersed in a toluene bath and thermostated within an error of ± 0.1 °C.

2.4.2. Stability measurements

Stability measurements were performed with separation analyser LUMiFuge 114 (L.U.M. GmbH, Germany). Measurements were made in glass tubes at acceleration velocities from 500 to 3000 rpm. The slope of sedimentation curves was used to calculate the sedimentation velocity and to get information about stability of the samples.

2.4.3. Scanning electron microscopy (SEM)

SEM images were taken with Gemini microscope (Zeiss, Germany). Samples were prepared in the following manner. Dispersions were diluted with deionized water, dropped onto aluminium support and dried at room temperature. Samples were coated with thin Pd layer to increase the contrast and quality of the images. Pictures were taken at voltage of 4 kV.

2.4.4. ξ-potential measurements.

ξ-potential measurements have been performed with Zetasizer 2000, Malvern Instruments. pH was adjusted by addition of 0.01 M NaOH or 0.001 M HCl. Average value of at least 10 measurements was adopted as ξ-potential at certain pH value.

2.4.5. Thermo gravimetrical analysis (TGA)

To determine the iron oxide content in composite particles the TGA 7 Perkin Elmer instrument (Pyris-Software Version 3.51) was used. Before measurement samples were dried in vacuum for ca 48 h. Samples were analyzed in closed aluminium cups in temperature range 25–600 °C (heating rate 5 K/min in nitrogen atmosphere).

2.4.6. Magnetization measurements

The vibrating-sample magnetometer (VSM Oxford) was used to study the magnetic properties of composite particles with a maximum magnetic field of 1 T at 290 K.

2.4.7. X-ray diffraction measurements

XRD spectra of the composite iron oxide-containing particles were recorded with Siemens P5005 powder X-ray diffractometer equipped with a Cu Kα (wavelength 1.540 Å) radiation source using the Diffracplus software.

3. Results and discussion

3.1. Preparation of iron oxide nano-particles

Preparation of magnetic nano-particles has been performed by standard procedure which includes reaction of Fe^{2+} and Fe^{3+} in aqueous medium at basic pH without presence of oxygen [13]. Typically, very small iron oxide particles have been obtained (10–20 nm) which can be clearly seen in SEM image in Fig. 1.

Obtained iron oxide particles did not form stable dispersion in water and precipitate with time. Dynamic light scattering measurements presented in Fig. 2 show giant aggregates around 1 μm in diameter present in aqueous medium.

After treatment with sodium oleate it was possible to obtain quite stable dispersion in water and DLS measurements indicate that separate iron oxide particles are present in solution and also some fraction of aggregates with average diameter 150 nm are still existing. This observation indicates that sodium oleate molecules stabilize effectively iron oxide particles and prevent aggregate formation in the system.

ξ-potential measurements presented in Fig. 3 indicate clearly that adsorption of sodium oleate on the surface of iron oxide particles changes considerably the position of isoelectric point (shift from 7.3 to 4). This leads to the domination of the negative charge on the iron oxide surface in the broader pH range.

3.2. Synthesis of hybrid PS-AAEM-Fe_3O_4 particles

3.2.1. Not treated iron oxide

Emulsion polymerization of styrene (ST) and acetoacetoxyethyl methacrylate (AAEM) has been performed in presence of different amounts of iron oxide particles. The attempt to perform polymerization with persulfate initiator led to limited conversion and such effect was more

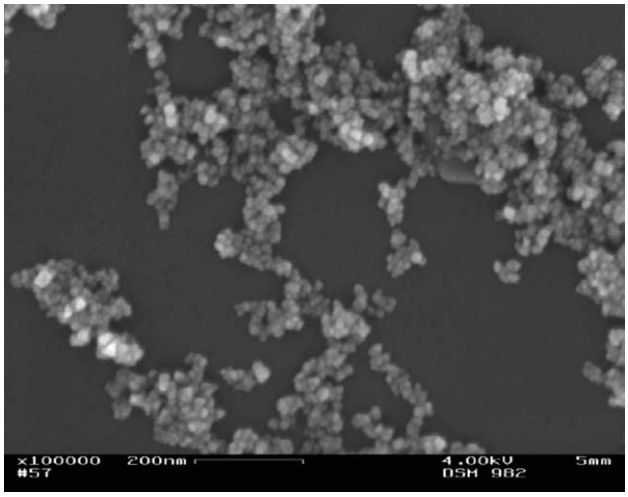

Fig. 1. SEM images of iron oxide nano-particles.

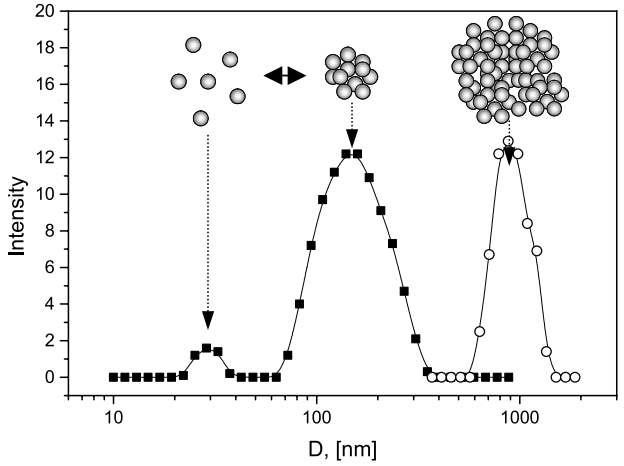

Fig. 2. DLS spectrum of bare iron oxide particles (open symbols) and coated with sodium oleate (solid symbols).

pronounced if the iron oxide amount in reaction mixture was raised up. The reason for limited conversion in this case is probably the deactivation of radical-anions originating after persulfate decomposition by iron oxide particles which bear strong positive charge at polymerization pH 3–4 (see Fig. 3). By using water-soluble azo-initiator it was possible to perform polymerization process to high conversion independently on the iron oxide amount in the system. But obtained latexes show time-dependent phase separation and black precipitate was formed on the bottom of the flask. Closer look at the morphology of obtained particles can explain such effect. Fig. 4 shows SEM pictures of obtained particles.

It is obvious that addition of the iron oxide to the reaction system influences dramatically the polydispersity of the formed particles if to compare with PS/AAEM microspheres prepared at similar conditions. It is also clear that there is no effective incorporation of magnetic particles into polymeric spheres during polymerization process. Iron oxide particles are even not distributed on the polymer

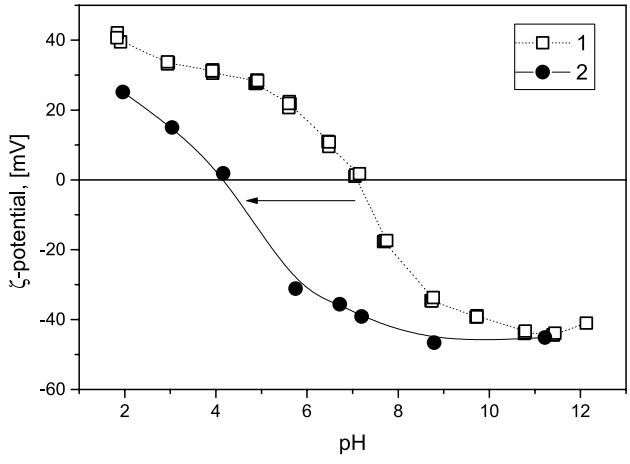

Fig. 3. ξ-potential of magnetic particles as a function of pH (1-iron oxide; 2-iron oxide after coating with sodium oleate).

particle surface, but aggregate and build large domains, and this is naturally a reason for precipitation, which was mentioned above. At the same time PS/AAEM particles are quite stable and no precipitation can be observed for long time. From these results we can conclude that in present system formation of the composite particles does not takes place and it seems that iron oxide particles disturb the nucleation process in the system. It is possible to assume that there is a strong repulsion forces between positively charged magnetic particles (reaction pH 3–4) and growing polymeric particles which bear also some positive charges originating from azo-initiator fragments. This effect probably hinders the encapsulation of the magnetic particles into polymeric matrix.

Average particle diameters of obtained particles measured by DLS are summarized in Table 1. Three particle generations can be detected and the middle peak correlates with the particle size of original PS/AAEM particles. Formation of smaller particles is probably induced by presence of magnetic nano-particles, which can stabilize some monomer at the initial stages of emulsion polymerization and provide formation of new nucleation cites. The large particles observed in DLS are aggregates consisting of polymeric particles and iron oxide which are clearly seen in SEM images.

Sedimentation velocity of the formed particles is not changed by presence of iron oxide in the system. But it should be noted that the values reported in Table 1 correspond mostly to sedimentation of polymeric particles. Aggregates of magnetic particles precipitate very rapidly and due to the much slower sedimentation of polymeric beads and high turbidity this process cannot be detected by the separation centrifuge. So, obtained sedimentation velocity values does not reflect completely the behaviour of the system but can be compared with results obtained for particles prepared with sodium oleate coated iron oxide which will be discussed in next chapter.

3.2.2. Iron oxide treated with sodium oleate

In this set of experiments emulsion polymerization of styrene and acetoacetoxyethyl methacrylate has been performed in presence of different amounts of iron oxide particles modified by sodium oleate. In this case we obtained stable lightly yellow latexes and no phase separation was observed (see Fig. 5)

This effective encapsulation of iron oxide is due to the modification of the iron oxide particles by sodium oleate. As it was mentioned earlier, modification of the iron oxide by sodium oleate causes following effects. Firstly, iron oxide particles are better redispersed in aqueous phase e.g. less aggregate formation was observed. This is due to the stabilizing effect of sodium oleate molecules, which are adsorbed onto iron oxide particle surface. This process leads also to the modification of the inorganic particle surface and it becomes more hydrophobic and additionally isoelectric point is shifted to lower pH values (see Fig. 3). Therefore, at

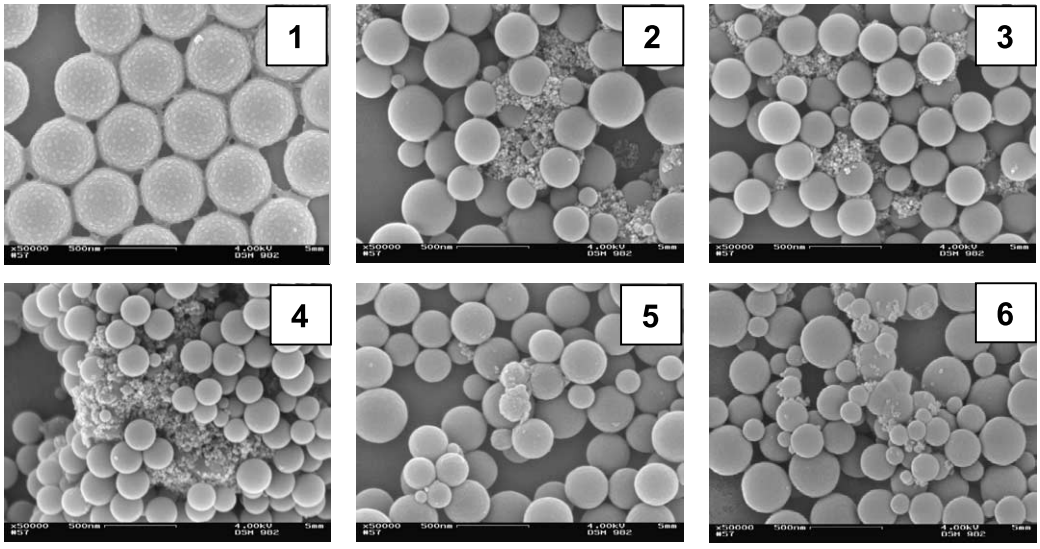

Fig. 4. SEM images: (1) PS-AAEM core and particles prepared at different iron oxide contents: (2) 1%; (3) 2%; (4) 3%; (5) 6%; (6) 8%.

polymerization conditions (pH = 4) iron oxide particles coated with sodium oleate possess very weak charge and hydrophobic surface what induces effective incorporation into hydrophobic polymer matrix.

SEM images presented in Fig. 6 indicate that in present system effective encapsulation of magnetic particles takes place and particles with interesting morphology have been formed. As in the case of non-modified iron oxide particles addition of inorganic component increases the polydispersity of the system, but this effect is more pronounced at high iron oxide contents. No bare iron oxide particles can be found beside composite particles. Starting from 8% iron oxide content in the system small inclusions appears on the surface of PS/AAEM beads and their number increases continuously. Careful examination of these inclusions by EDX technique confirms presence of Fe inside. We suppose that iron oxide is distributed not only inside of the PS/AAEM particles but also outside in form of discrete domains coated with polymeric shell. To confirm this idea TEM measurements will be performed in the near future. The origin of such interesting 'pickering' morphology is perhaps the simultaneous formation of large PS/AAEM composite beads and small particles with iron oxide core and polymeric shell which precipitate on the surface of larger spheres during polymerization process.

Table 2 shows the results of TGA analysis which indicate that composite particles with various iron oxide contents have been prepared. The sedimentation velocity of composite particles is much higher as reported previously in Table 1 and measured value increases if the iron oxide content is rising up.

DLS measurements do not show any correlation of the particle size with iron oxide content in composite particles. But it is clear from SEM images presented in Fig. 5 that the particle size remains more or less constant and more and smaller particles are produced at higher contents of magnetic particles.

The next experiment set was performed to investigate the influence of AAEM content on the final size and morphology of composite particles. The iron oxide particle concentration in reaction mixture was kept constant (16% of the monomer weight) and AAEM concentration was varied from 2.5 to 10% (relatively to styrene weight). In our previous study it was found that increase of AAEM concentration in reaction mixture with styrene as main monomer leads to formation of smaller PS/AAEM particles

Table 1
DLS and sedimentation velocity data of obtained particles

Sample	Iron oxide content, [%]	D^{DLS}, [nm]			Sed vel[a] [μm/sek]
		Peak1	Peak2	Peak3	
1	0	–	550	–	5.877
2	1	–	468.1	7898.2	0.861
3	2	142.3	481.4	6893.1	0.780
4	3	–	285.5	–	0.582
5	6	112.7	503.76	3237.9	0.677
6	8	152.6	604.6	3364.2	0.619

[a] 2000 rpm.

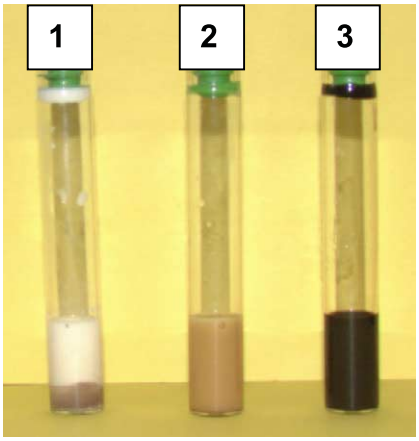

Fig. 5. Photographs of latexes obtained with: (1) non-modified iron oxide and (2) iron oxide modified by sodium oleate; iron oxide dispersion (3).

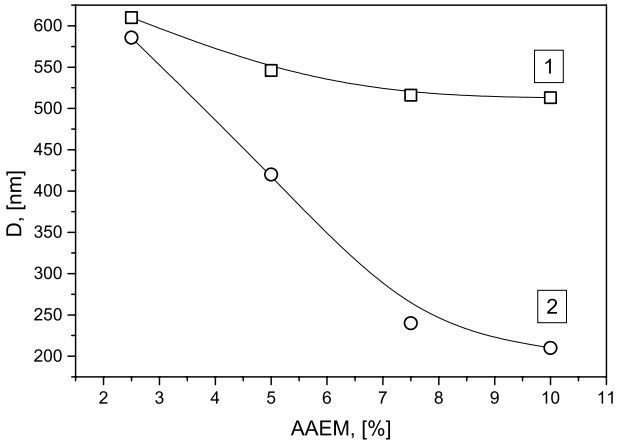

Fig. 7. Average particle diameter of PS-AAEM particles (1) and corresponding iron oxide-containing particles (2) prepared at different AAEM contents (iron oxide content ca. 16%).

[7]. The average diameter of PS/AAEM particles and corresponding composite particles with iron oxide prepared at different AAEM concentrations are shown in Fig. 7.

It is obvious from Fig. 7 that increase of AAEM content leads to decrease of final particle size due to the hydrophilic character of AAEM it can provide some sterical stabilization to formed particles. However, increase of AAEM content in presence of iron oxide particles leads to much rapid decrease of the particle size comparing with non-magnetic analogues. It can be assumed that iron oxide particles participate actively in nucleation process providing new nucleation sites and sufficient stabilization for growing particles. This leads to rapid decrease of the particle size and increase of the particle number in the system. It is interesting to note that particle morphology in also changing. Fig. 8 shows SEM images of hybrid particles prepared at 5 and 10% AAEM.

Increase of AAEM concentration in reaction mixture leads to formation of small particles without Pickering morphology. It should be noted that increase of AAEM content did not improve strongly the polydispersity of the system. Sedimentation tests indicate that composite particles prepared at different AAEM contents are quite stable in aqueous medium and show no precipitation for at least 4 month.

Obtained composite particles were characterized with respect to their magnetic properties. Magnetization curves for particles bearing different iron oxide contents are presented in Fig. 9. The magnetic response to external field increases if the iron oxide amount encapsulated in PS/

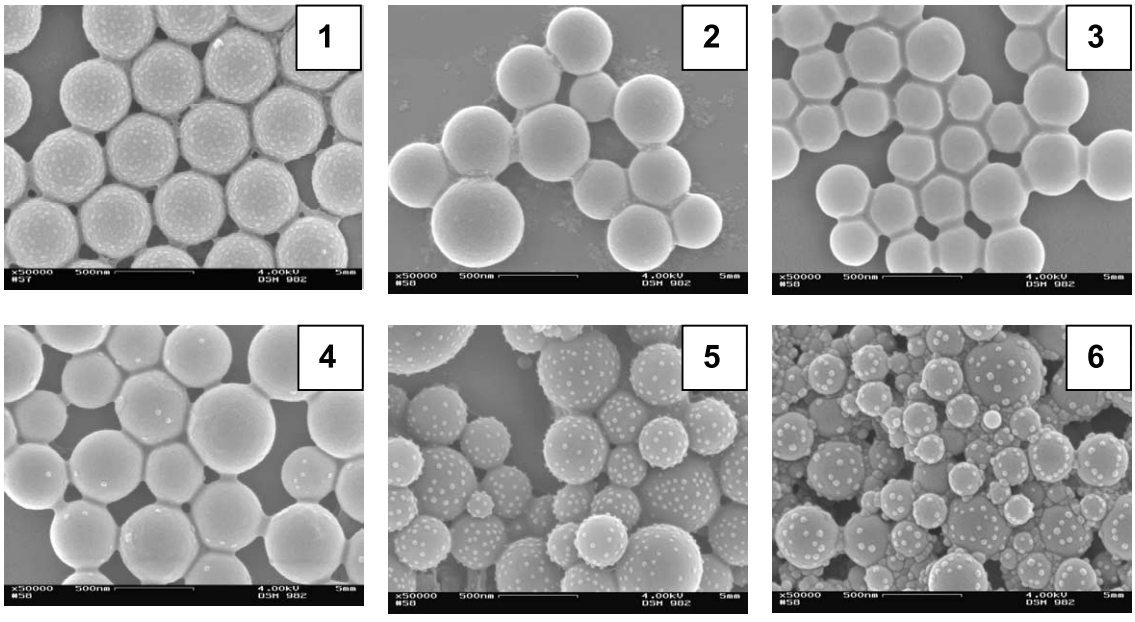

Fig. 6. SEM images of PS-AAEM core (1) and composite particles prepared with different iron oxide contents: (2) 2%; (3) 6%; (4) 8%; (5) 16%; (6) 20% (AAEM content 5%).

Table 2
DLS and sedimentation velocity data of obtained particles

Sample	Iron oxide content, [%]	TGA, [%]	D^{DLS},[nm]	Sed vel[a] [μm/sek]
1	0	0	550	5.88
2	2	7.59	515	7.69
3	4	6.77	502	8.45
4	6	9.87	469	10.09
5	8	12.32	555	16.64
6	16	13.89	470	16.20
7	20	15.23	407	15.19

[a] 2000 rpm.

AAEM particles is rising up. This plot demonstrates that it is possible to control the magnetic properties of composite particles simply by controlling the initial concentration of magnetic nano-particles in the reaction mixture.

X-ray diffraction spectra of composite particles show existence of characteristic peaks of iron oxide indicating presence of this inorganic material in hybrid particles. Shown in Fig. 10 are the locations of expected Bragg reflections (solid lines) and peaks at the 2θ angles of 30.1° (d = 2.962 Å); 35.6° (d = 2.522 Å); 43.4° (d = 2.083 Å); 53.9° (d = 1.606 Å); 59.8° (d = 1.546 Å); and 62.4° (d = 1.487 Å) corresponding to γ-Fe_2O_3 crystalline structure. The reflection peaks in 30–70° region are quite similar to those of the γ-Fe_2O_3 reported by other groups [14–17]. The intensity of the peaks in the spectrum of composite particles is much smaller comparing with bare iron oxide particles due to the presence of polymeric material.

It has been reported by different authors that preparation of iron oxide by reaction of Fe^{2+} and Fe^{3+} in basic conditions can lead to formation of mixture of different iron oxides such as iron oxide (Fe_2O_3), hematite (α-Fe_2O_3), maghemite (γ-Fe_2O_3) or even ferric hydroxide

(β-FeOOH) which all possess magnetic properties [7,19]. This effect depends strongly on reaction conditions and purity of the ingredients. Presence of oxygen can lead to oxidation of Fe_3O_4 as given by the following equations [18]:

$$Fe_3O_4 + 0.25O_2 + 4.5\ H_2O \rightarrow 3\ Fe(OH)_3 \quad (5)$$

$$Fe_3O_4 + 0.25\ O_2 \rightarrow 1.5\ Fe_2O_3 \quad (6)$$

Eq. (6) shows transformation of iron oxide into maghemite in presence of oxygen molecules. This reaction can take place directly during reaction of Fe^{2+} and Fe^{3+} in basic aqueous solution or later during emulsion polymerization step induced by high temperatures and oxidizing effect of persulfate initiator and some oxygen present in aqueous medium.

4. Conclusions

Particle preparation by surfactant-free emulsion polymerization of styrene (ST) and acetoacetoxyethyl methacrylate (AAEM) in presence of magnetic nano-particles is described. It has been established that the modification of the iron oxide nano-particle surface with sodium oleate improves significantly the encapsulation of iron oxide during polymerization process. This procedure gives a possibility to obtain composite particles with pickering morphology and both the particle size and iron oxide content can be varied. Up to 15% iron oxide was encapsulated in PS/AAEM particles. Variation of monomer to iron oxide ratio gives a possibility to change the morphology of hybrid particles; however, composite particles with broader particle size distribution have been obtained at higher content of magnetic particles in the system. Increase of AAEM concentration in reaction mixture induces decrease of the particle size from 600 to 200 nm at constantly high iron oxide content (ca. 16%). This is an important achievement since small particles combining

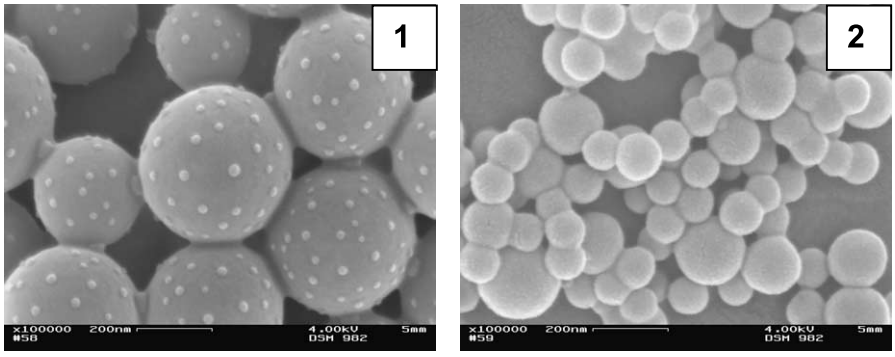

Fig. 8. SEM images of hybrid particles prepared with 5% (1) and 10% (2) AAEM (iron oxide content ca.16%).

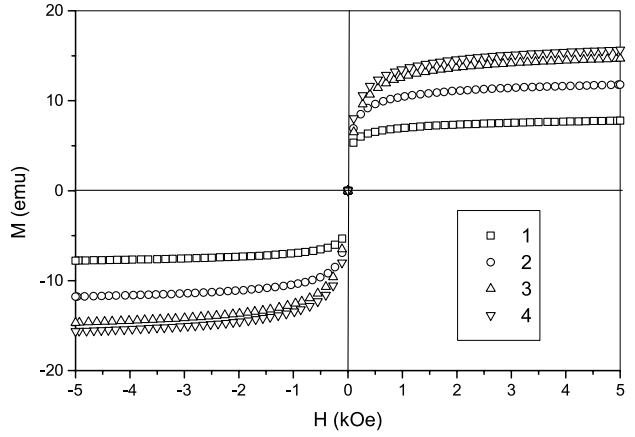

Fig. 9. Magnetization curves of composite PS/AAEM particles with different iron oxide contents (1–9.87%; 2–12.32%; 3–13.89%; 4–15.23%).

magnetic properties and reactive groups on the surface are of particular interest as they offer a large specific surface area for binding of biomolecules. Composite particles were characterized by dynamic light scattering and electron microscopy (SEM) with respect to their particle size and morphology of the surface layer. X-ray diffraction (XRD)

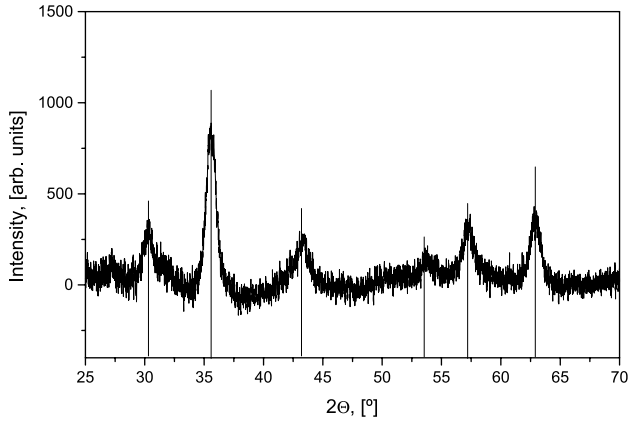

Fig. 10. XRD spectra of composite PS/AAEM particles (iron oxide content—15.23%).

and magnetization measurements confirm presence of iron oxide (γ-Fe_2O_3) in composite microspheres.

Acknowledgements

The authors are thankful to Mrs E. Kern for SEM measurements, Dr Yu. Prots for XRD measurements. Many thanks to Deutsche Forschungsgemeinschaft (DFG) with collaboration research project SFB 287 ‘Reactive Polymers’ and DAAD Masters Sandwich Programme with IIT Delhi for financial support.

References

[1] Elaissari A, Sauzedde F, Montagne F, Pichot C. In: Elaissari A, editor. Colloidal polymers: synthesis and characterization. New York: Marcel Dekker; 2003. p. 285–318.
[2] Ugelstad J, Kaggeurd KH, Hansen FK, Berg A. Makromol Chem 1979;180:737.
[3] Ugelstad J, Mork PC, Kaggeurd KH, Ellingsen T, Berg A. Adv Colloid Interface Sci 1980;13:1201.
[4] Caruso F, Caruso FA, Möhwald H. Science 1998;282:1111.
[5] Caruso F, Spasova M, Susha A, Giersig M, Caruso FA. Chem Mater 2001;13:109.
[6] Furusawa K, Nagashima K, Anzai C. Colloid Polym Sci 1994;272: 1104.
[7] Sauzedde F, Elaissari A, Pichot C. Colloid Polym Sci 1999;277:846.
[8] Sauzedde F, Elaissari A, Pichot C. Colloid Polym Sci 1999;277:1041.
[9] Dresco PA, Zaitsev VS, Gambino RJ, Chu B. Langmuir 1999;15: 1945.
[10] Gu S, Shiratori T, Konno M. Colloid Polym Sci 2003;281:1076.
[11] Lansalot M, Pichot C, Elaissari A. PDM-2004 Abstract Book, 2004. p. 239–242.
[12] Pich A, Bhattacharya S, Adler HJ. Polymer 2005;46:1077.
[13] Buske N, Sonntag H, Götze T. Colloid Surf 1984;12:195.
[14] Sohn BH, Cohen RE. Chem Mater 1997;9:264.
[15] Kobayashi Y, Kawashima D, Tomita A. Chem Mater 1997;9:1887.
[16] Nguyen T, Diaz A. Adv Mater 1994;6:858.
[17] Xiaotun Y, Lingge X, Choon NS, Hardy CSO. Nanotechnology 2003; 14:624.
[18] Kim DK, Mikhaylova M, Zhang Yu, Muhammed M. Chem Mater 2003;15:1617.
[19] Huang Z, Tang F. J Colloid Interface Sci 2004;275:142.